THEORETICAL STUDY OF THE CONFORMATIONAL BEHAVIOUR OF POLY(OXYPROPYLENE) CHAINS

Robert F. T. STEPTO and David J. R. TAYLOR

Polymer Science & Technology Group,
Manchester Materials Science Centre, University of Manchester and UMIST, Grosvenor Street,
Manchester M1 7HS, United Kingdom

Received March 29, 1995
Accepted June 28, 1995

Dedicated to Dr Blahoslav Sedlacek on the occasion of his 70th birthday.

***B** e this a story told, of*
***L** eft and right most bold,*
***A** lthough acrostic in this part.*
***H** aving weights from the start*
***O** xypropylene does grow,*
***S** cientists will surely know.*
***L** eaning this way, then that*
***A** tactic but not flat,*
***V** ivat physics and its Pop.*

The present paper describes the calculation of the conformational behaviour of isotactic, syndiotactic and atactic poly(oxypropylene) (POP) chains, using rotational-isomeric-state (R-I-S) theory in the form of BIOSYM's *Polymer* computer-software. It is found that the conformational behaviour of the POP chain, in the region of an *R* methyl-substituted skeletal carbon atom, differs from that in the region of the corresponding *S* carbon, due to the differences in the steric interactions between the methyl side-group and the methylene group two skeletal atoms away in the POP backbone. Thus, the isotactic and syndiotactic chains have markedly different values of C_n, the characteristic ratio. Accordingly, C_n was calculated for isotactic, syndiotactic and atactic POP chains of various numbers of skeletal bonds, n. The results showed that the isotactic chains occupy more extended conformations (with the highest values of C_n), compared with the highly-coiled syndiotactic chains (lower values of C_n). For the atactic POP chains, C_n was found to lie between the two extremes of the isotactic and syndiotactic forms. The value of C_∞ for the infinite atactic POP chain was found to be consistent with values determined from experimental measurements.

The present interest in the conformational behaviour of poly(oxypropylene) (POP) chains stems from the use of essentially atactic POP triols and tetrols in gelation and network studies[1], using polyurethane- and polyester-forming polymerisations. The mean-square end-to-end distance, $\langle r^2 \rangle$, of a linear POP chain of a given number of

skeletal bonds, n, is an important parameter characterising intramolecular reaction and, hence, delay in gel point and network defects[1].

A measure of chain-flexibility is provided[2] by the characteristic ratio, C_n,

$$C_n = \frac{\langle r^2 \rangle}{n\langle l^2 \rangle} \quad , \qquad (1)$$

where $\langle l^2 \rangle$ is the mean-square skeletal-bond length. In relation to the gelation and network studies[1], values of C_n for atactic POP chains at the reaction temperatures of 333 K and 353 K, with n in the range 15 to 150 skeletal bonds, are required.

To the authors' knowledge, no experimental measurements of the dimensions of atactic POP chains, of the required lengths and at the required temperatures, have been reported in the literature[3]. A theoretical study of the conformational properties of POP chains was carried out by Abe, Hirano and Tsuruta[4]. This work involved the semi-empirical determination of a set of conformational energies associated with bond-rotations along the POP-chain backbone, in order to reproduce, using rotational-isomeric-state (R-I-S) theory[2], experimentally determined[5,6] values of $\langle r^2 \rangle$ for supposedly isotactic, high molar-mass POP.

For the current work, it was decided that the evaluation of C_n for atactic POP would be approached theoretically, using R-I-S theory, with POP-chain-conformational energies, and hence statistical weights and preferred rotational-angles, based on the atomic potential-energy functions in a commercially-available forcefield[7] (see later). Hence, their values should be independent of the somewhat arbitrary, empirical deductions used previously[4]. The theoretical methods developed, which include an analysis of isotactic and syndiotactic POP chains, and the results obtained form the basis of the present communication.

The calculations used BIOSYM's *Polymer* software[7], employing *Insight II* version 2.3.0 as the user-interface, and the "Polymerizer", "R-I-S" and "Discover" modules. They were carried out on a Silicon Graphics *Indy* workstation (*Indy* 24 bit, 100 MHz processor, 32 MB memory, IRIX 5.2).

Definition of Chain Model and Tacticity

The POP repeat unit consists of three skeletal bonds connecting methylene carbon, methyl-substituted carbon and oxygen atoms as shown in Fig. 1. It is immediately apparent that the POP repeat unit shows stereoisomerism, due to the presence of the asymmetric, methyl-substituted carbon atom (*C). Thus, POP chains are subject to the effects of tacticity, due to the occurrence of the two isomeric forms of the *C atoms along the polymer backbone. The two isomers may be denoted *R* and *S*, dependent[8] upon the cyclic order of the placement of the four atoms pendant to *C. If the *C atom

is viewed along the *C–H bond, with the H atom facing away from the observer, the three remaining atoms attached directly to *C can be arranged in order of priority, based on the atomic numbers of the pendant atoms[8]. If their atomic numbers decrease in a clockwise direction, the asymmetric carbon is denoted *R*; conversely, a decrease in an anti-clockwise direction is indicative of the *S* form. If two or more of the pendant atoms are identical, the test for priority is extended to the next atom in the side group, until a definite order of priority can be established. For the POP chains in the present investigation, the highest priority atom attached directly to *C, is, therefore, the O atom; the pendant atom of next highest priority is the backbone-methylene carbon (it also has the polymer chain attached), and the atom of lowest priority is the pendant-methyl carbon. The designation of *R* and *S* isomers is shown schematically in Fig. 2.

An isotactic POP chain is made up of *C atoms of a single isomeric form (all *R*, or all *S*), whereas the syndiotactic chain consists of alternating *R* and *S* forms. In an atactic POP chain, the *R* and *S* forms of *C occur completely at random. Sections of isotactic

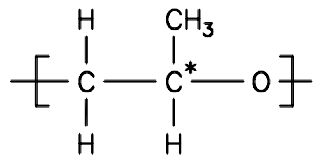

FIG. 1
Chemical structure of the poly(oxypropylene) (POP) repeat unit. *C denotes the asymmetric carbon atom

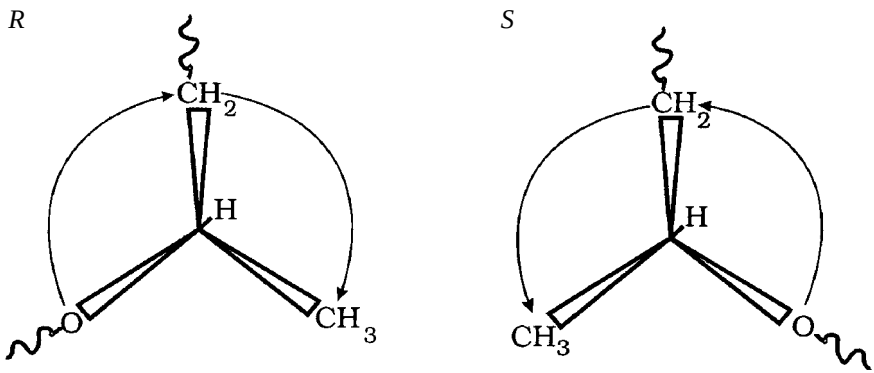

FIG. 2
Description of the *R* and *S* isomers of the asymmetric carbon atom in the POP backbone

and syndiotactic POP chains, in all-trans chain-conformations, are shown in Fig. 3. It is interesting to note that[9], because asymmetric carbon atoms are three (or an odd number of) skeletal bonds apart, the methyl side-groups of the isotactic POP chain are staggered on opposite sides of the chain backbone (typical of a syndiotactic chain with asymmetric C atoms an even number of backbone bonds apart, such as polypropylene or polystyrene). Conversely, the syndiotactic POP chain has methyl side-groups arranged on the same side of the chain backbone (typical of isotactic polypropylene or polystyrene).

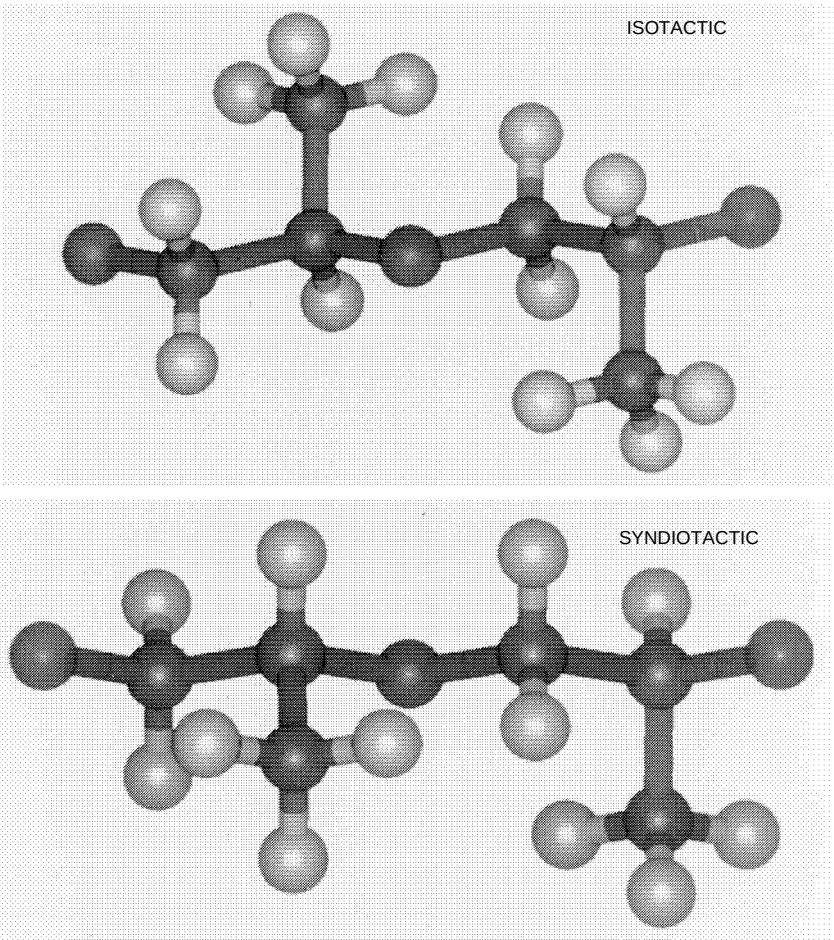

FIG. 3
Three-dimensional views of sections of isotactic (-*R*-*R*-*R*-*R*-)- and syndiotactic (-*R*-*S*-*R*-*S*-)-POP chains in chain-extended, planar-trans conformations. C atoms are coloured green, O atoms red, and H atoms brown

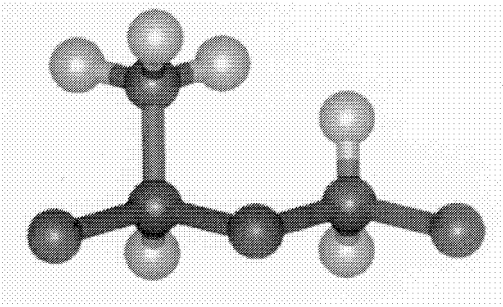

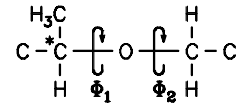

fragment **1**

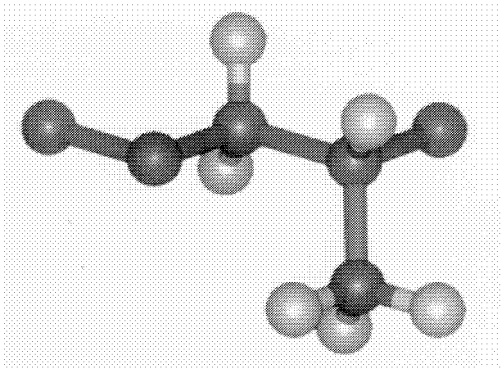

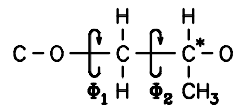

fragment **2**

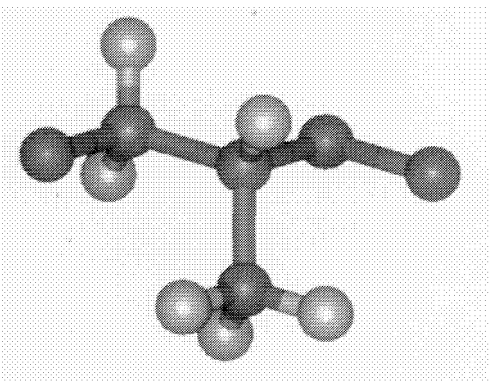

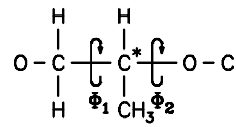

fragment **3**

FIG. 4

The set of *R*-POP fragments for the R-I-S calculation of potential-energy surfaces associated with the sequential dihedral angles ϕ_1 and ϕ_2. Atomic colour-coding as for Fig. 3

R-I-S Analysis

Potential Energy Surfaces

The first stage in the R-I-S analysis involved the determination of the preferred rotational (dihedral) angles for sequences of three skeletal bonds, and their associated statistical weights[2]. This was achieved by breaking the POP chain-structure into three "fragments", each fragment consisting of two sequential groups of three skeletal bonds (i.e. four skeletal bonds). The set of three (*R*) chain fragments is shown in Fig. 4. The rotational (potential) energy as a function of the two sequential dihedral angles, ϕ_1 and ϕ_2, denoted $E(\phi_1,\phi_2)$ was calculated, to generate a two-dimensional energy-contour map for both *R* and *S* forms of the *C atom in each fragment. The calculations were performed using the "R-I-S module" of BIOSYM's *Polymer* software[7] (*Insight II* version 2.3.0, *Discover* version 2.3.5) based on the CVFF forcefield[7], on the BIOSYM software default-option of no atomic changes, and on the default-values of bond lengths, l_{O-C} = 0.143 nm, l_{C-C} = 0.154 nm, l_{C-H} = 0.107 nm, and valence-angle supplements, $\theta_O = \theta_C = 70.5°$.

The resulting set of maps is shown in Fig. 5. $\phi_i = 0°$ defines the planar-trans conformation of three skeletal bonds, with positive angles indicating a right-handed bond-rotation[2,7] (i.e. a rotation which would increase the distance between the pair of groups, if the bond joining them were a right-hand screw, with the skeletal atoms threaded to it). An example of a three-dimensional potential-energy surface, in this case for fragment 3*R*, which has six energy-minima, is shown in Fig. 6.

Statistical Weights and Preferred Conformers

The number and positions of the energy minima of a given contour map yield the values of the preferred pairs of R-I-S dihedral-angles for that particular fragment. The partition functions, at an absolute temperature, *T*, for each local minimum and its surrounding region, are determined[7] by numerical evaluation of the following integrals,

$$z_{tot} = \int_{\phi_2}\int_{\phi_1} \exp\left[-E_{tot}(\phi_1,\phi_2)/RT\right] \mathrm{d}\phi_1 \, \mathrm{d}\phi_2 \qquad (2)$$

and

$$z_{net} = \int_{\phi_2}\int_{\phi_1} \exp\left[-E_{net}(\phi_1,\phi_2)/RT\right] \mathrm{d}\phi_1 \, \mathrm{d}\phi_2 \ ; \qquad (3)$$

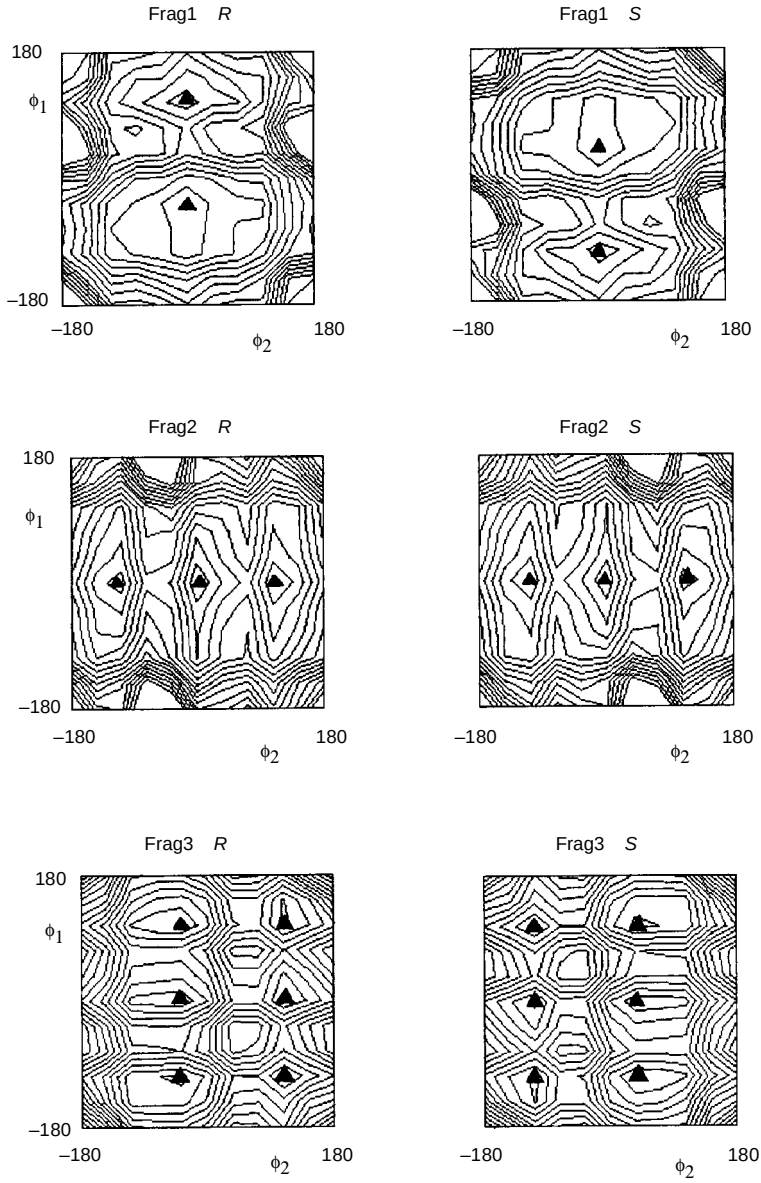

FIG. 5

Two-dimensional potential-energy contour-maps associated with the dihedral angles ϕ_1 and ϕ_2, for both *R* and *S* forms of the three POP chain-fragments (Frag1, Frag2 and Frag3) of Fig. 4. Contours are shown at fifteen intervals (of 4.184 kJ mol^{-1}) beginning at the minimum energies (▲) of each map

z_{tot} is the partition function defined on the basis of the total potential-energy of the region, whereas z_{net} is that based only upon the net potential-energy, $E_{net}(\phi_1,\phi_2)$. The latter is calculated by subtraction of the energy, $E(\phi_1)$, associated with the ϕ_1 dihedral angle, from the total energy[7]:

$$E_{net}(\phi_1,\phi_2) = E_{tot}(\phi_1,\phi_2) - E(\phi_1) \quad . \tag{4}$$

The preferred (average) values of ϕ_1 and ϕ_2 and the average net energy, $<E_{net}>$, of each region in which a minimum exists are then determined as

$$<\phi_k> = z_{tot}^{-1} \int_{\phi_2}\int_{\phi_1} \phi_k \exp\,[-E_{tot}(\phi_1,\phi_2)/RT]\mathrm{d}\phi_1\,\mathrm{d}\phi_2 \quad , \quad k = 1, 2 \quad , \tag{5}$$

and

$$<E_{net}> = z_{net}^{-1} \int_{\phi_2}\int_{\phi_1} E_{net}(\phi_1,\phi_2) \exp\,[-E_{net}(\phi_1,\phi_2)/RT]\mathrm{d}\phi_1\,\mathrm{d}\phi_2 \quad . \tag{6}$$

The $<\phi_1>$ and $<\phi_2>$ for the various regions define up to three distinct values, giving gauche$^-$ (g^-), trans (t) and gauche$^+$ (g^+) rotational states for each of ϕ_1 and ϕ_2. However, the value of ϕ_{g-}, ϕ_t, or ϕ_{g+} for a given bond from various regions may be slightly different. Hence, the values of ϕ_{g-}, ϕ_t and ϕ_{g+} are each averaged according to the total partition functions of the regions concerned, to define single values of ϕ_{g-}, ϕ_t and ϕ_{g+}, which become the dihedral angles for subsequent R-I-S matrix calculations[2]. The different values of the dihedral angles (rotational states) of a bond pair may be denoted (i, j), with i, j = {g^-, t, g^+}. The normalised statistical weight of state (i, j) is then defined as

$$u_{i,j} = \frac{(z_{net})_{i,j}}{(z_{net})_{ref}} \quad , \quad \text{or} \quad u_{i,j} = 0 \quad , \tag{7}$$

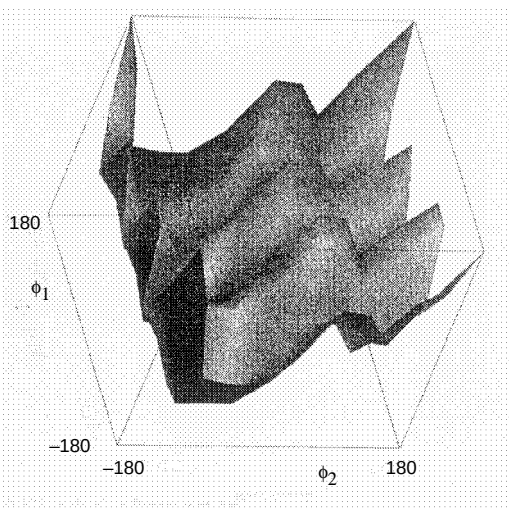

FIG. 6
Three-dimensional potential-energy surface for POP-chain fragment 3*R*. Six energy-minima are evident; the (vertical) potential-energy axis runs from 15.1 to 77.0 kJ mol^{-1}

$(z_{net})_{i,j}$ is the partition function of the region around (i, j), according to Eq. (*3*), and $(z_{net})_{ref}$ is the corresponding partition function of the region of minimum $<E_{net}>$, as evaluated through Eq. (*6*). If a region has no energy minimum, $u_{i,j} = 0$. It may be noted that the values of ϕ_1 and ϕ_2 are also made consistent between successive fragments (ϕ_2 for a given fragment becomes ϕ_1 for the next fragment along in the chain).

The resulting set of preferred R-I-S dihedral angles for each POP chain fragment, and the associated normalised statistical-weight matrices, $\boldsymbol{U} = [u_{i,j}]$, at 298 K, are listed according to the following scheme[7].

$$\begin{array}{cc} & \begin{array}{ccc} \phi_2 & & \\ g^- & t & g^+ \end{array} \\ \phi_1 \begin{array}{c} g^- \\ t \\ g^+ \end{array} & \left[\begin{array}{ccc} & & \\ & & \\ & & \end{array}\right] \end{array}$$

a) fragment 1 $\quad$ — CH_2 — $^*CH(CH_3)$ — O — CH_2 — $CH(CH_3)$ —

$\phi_1 \quad \phi_2$

R $\quad \phi_1 = -49.71°, 110.20° \quad \phi_2 = -3.11° \quad \boldsymbol{U} = \begin{bmatrix} 0 & 0.949 & 0 \\ 0 & 0 & 0 \\ 0 & 1.0 & 0 \end{bmatrix}$

S $\quad \phi_1 = -110.19°, 49.67° \quad \phi_2 = -2.56° \quad \boldsymbol{U} = \begin{bmatrix} 0 & 1.0 & 0 \\ 0 & 0 & 0 \\ 0 & 1.014 & 0 \end{bmatrix}$

b) fragment 2 $\quad$ — $CH(CH_3)$ — O — CH_2 — $^*CH(CH_3)$ — O —

$\phi_1 \quad \phi_2$

R $\quad \phi_1 = -2.56°$or $-3.11° \quad \phi_2 = -114.14°, 1.14°, 111.31° \quad \boldsymbol{U} = \begin{bmatrix} 0 & 0 & 0 \\ 0.462 & 0.820 & 1.0 \\ 0 & 0 & 0 \end{bmatrix}$

S $\quad \phi_1 = -2.56°$or $-3.11° \quad \phi_2 = -111.31°, -1.14°, 114.14° \quad \boldsymbol{U} = \begin{bmatrix} 0 & 0 & 0 \\ 1.0 & 0.819 & 0.462 \\ 0 & 0 & 0 \end{bmatrix}$

c) fragment 3 — O — CH_2 — $^*CH(CH_3)$ — O — CH_2 —
ϕ_1 ϕ_2

$$R \quad \phi_1 = -114.14°,\ 1.14°,\ 111.31° \quad \phi_2 = -49.71°,\ 110.20° \quad \boldsymbol{U} = \begin{bmatrix} 0.862 & 0 & 0.005 \\ 0.823 & 0 & 0.003 \\ 1.0 & 0 & 0.004 \end{bmatrix}$$

$$S \quad \phi_1 = -111.31°,\ -1.14°,\ 114.14° \quad \phi_2 = -110.19°,\ 49.67° \quad \boldsymbol{U} = \begin{bmatrix} 0.004 & 0 & 1.0 \\ 0.003 & 0 & 0.823 \\ 0.005 & 0 & 0.859 \end{bmatrix}$$

It is clear that ϕ_2 for a given fragment is ϕ_1 for the next fragment in the series. It is interesting that none of the chain fragments has a full compliment of g^-, t and g^+ preferred rotational angles, as seen from the zero-elements in the statistical-weight matrices. The dihedral angle of lowest average net energy for each of the POP chain-fragments is that for which $u_{i,j} = 1.0$. Normally, this means that the other statistical weights are less than unity. However, for fragment 1*S*, $u_{g+,t} = (z_{net})_{g+,t}/(z_{net})_{ref} = 1.014$, essentially because of the different shapes of the two energy minima.

The physical bases for the broad differences in the statistical weights associated with the values of ϕ_2 for a given fragment can be deduced by studying a model of the fragment concerned. Because the statistical weights for a given fragment are calculated using net energies (Eqs (*3*), (*4*) and (*7*)), they give a measure of the relative stabilities associated with the different ϕ_2-values for that fragment. The relative stabilities associated with the values of ϕ_1 for that fragment are elucidated by reference to the statistical weights for the previous fragment in the series (since ϕ_1 for any current fragment is ϕ_2 for the previous one). Considering first the set of *R* fragments in turn, the values of the preferred dihedral angles, and their statistical weights, can be rationalised as follows. Fragment 1*R* has only one preferred rotational state, $\phi_2 = -3.11°$ (trans), as illustrated in Fig. 7*a*, where the central bond for ϕ_2, CH_2–O, points into the page. Gauche states are disallowed, as they would give rise to second-order (pentane effect[2]), steric interactions between the $CH(CH_3)$ group, at the bottom in Fig. 7*a*, and either the $-CH_3$ side-roup or the backbone $-CH_2-$ group, both attached to the skeletal $^*C$ atom, and each situated four skeletal bonds away from the $CH(CH_3)$ group.

Moving on to fragment 2*R*, the fact that ϕ_1 is always trans (i.e. ϕ_2 for fragment 1*R* is always trans) means that side-group interactions are first-order only, due to rotation about the CH_2–$^*CH(CH_3)$ bond. Hence, only the three-bond sequence (O–CH_2–$^*CH(CH_3)$–O) defining ϕ_2 needs to be considered. It is shown in Fig. 7*b*, as Newman projections of the preferred conformers, gauche$^-$, trans, gauche$^+$. The relative statistical weights of these conformers can be rationalised in terms of the sizes of interacting

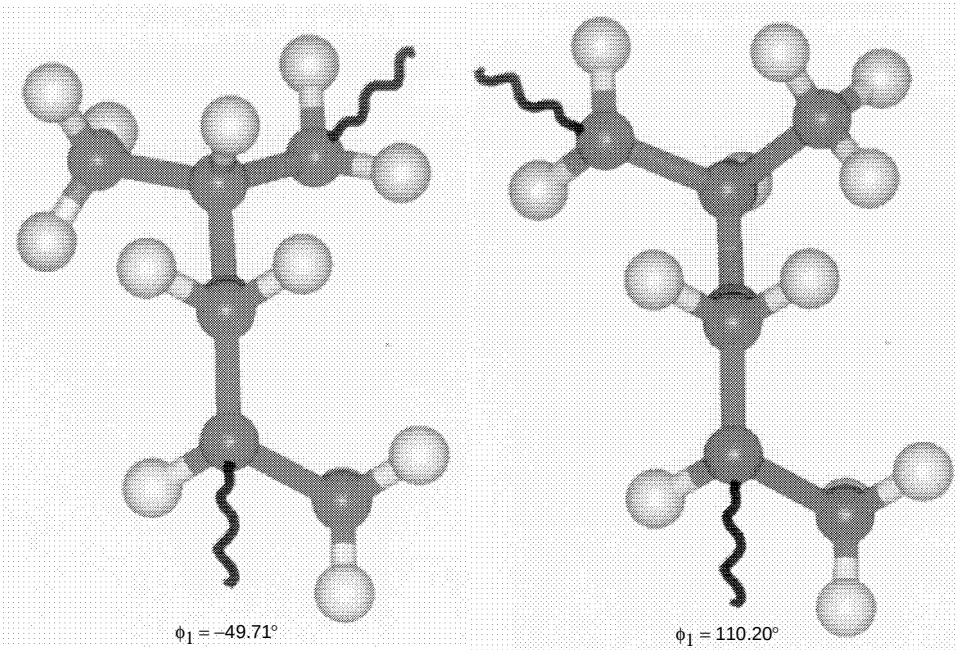

FIG. 7*a*

POP-chain fragment 1*R* in its two low-energy conformations. Rotation about the CH_2–O bond away from trans would result in second-order, steric interactions between the $CH(CH_3)$ group in the foreground, and the $–CH_3$ and $–CH_2–$ groups in the background. The most stable conformation is shown on the left, with $\phi_1 = -49.71°$. Atomic colour-coding as for Fig. 3

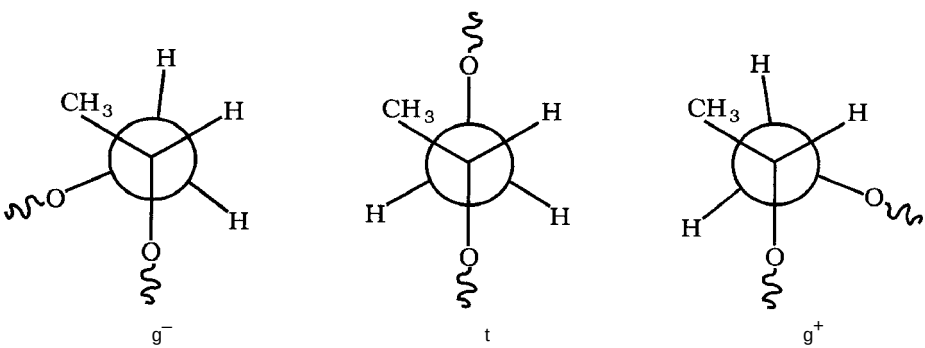

FIG. 7*b*

Newman projections of the ϕ_2 part of POP-chain fragment 2*R*. The g^-, t and g^+ conformations of the $O–CH_2–{}^*CH(CH_3)–O$ three-bond sequence. $\phi_{g-} = -114.14°$, $\phi_t = 1.14°$, $\phi_{g+} = 111.31°$

groups, as the effects of polarity have been ignored in the forcefield used. In reality, they must play a part. The most stable state ($u_{tg+} = 1.0$), corresponding to $\phi_2 = 111.31°$, coincides with a maximisation of the distance between the rear, skeletal –O– atom and the $–CH_3$ side-group, situated three bonds apart. Bond-rotation through to the trans state ($\phi_2 = 1.14°$) results in a closer approach between the –O–atom and the $–CH_3$ side-group, reducing the stability, and hence the statistical weight, of this bond conformation. Further bond-rotation, to the gauche$^-$ state ($\phi_2 = –114.14°$), results in the least stable bond-conformation (with the smallest statistical weight), due to increased O···O and O···CH_3 interactions. It may be noted that the relative stability of the (g^+) state of fragment 2*R* has been evaluated empirically by Abe et al.[4], to make calculated dimensions and dipole moments agree with selected experimental values. The relative stability is affected by the so-called gauche-oxygen effect, which occurs also in other polyoxide chains[10].

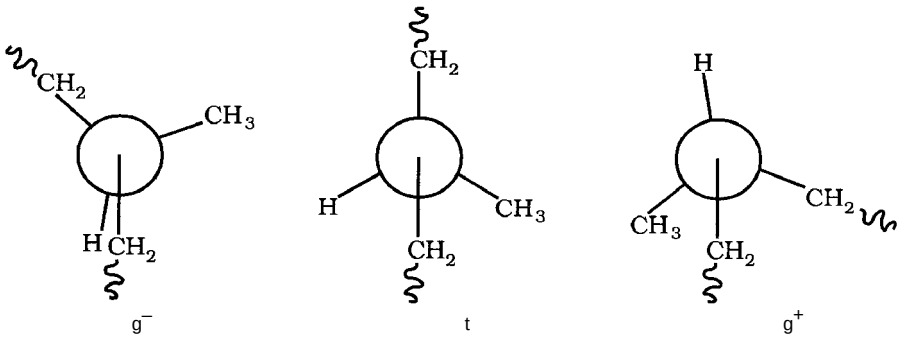

FIG. 7*c*

Newman projections of the ϕ_2 part of POP-chain fragment 3*R*. The g^-, t and g^+ conformations of the $CH_2–^*CH(CH_3)–O–CH_2$ three-bond sequence. $\phi_{g-} = –49.71°$, $\phi_t = 0°$ and $\phi_{g+} = 110.20°$

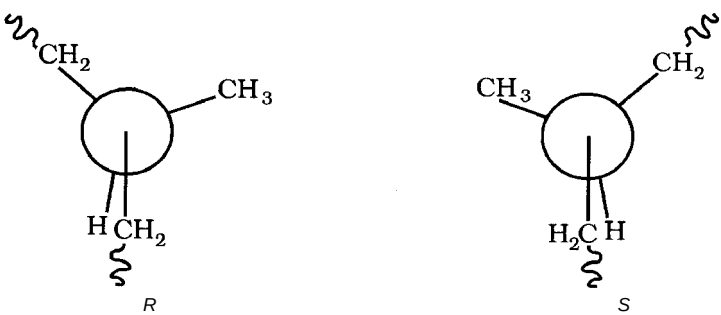

FIG. 7*d*

Newman projections of the ϕ_2 parts of POP-chain fragments 3*R* and 3*S* in their lowest-energy conformations, $\phi_{g-} = –49.71°$ and $\phi_{g+} = 49.67°$, respectively

In the present calculations it has arisen directly, although also somewhat empirically, from the forcefield used.

Finally, the interactions determining the preferred value of ϕ_2 for fragment 3*R* can be seen in terms of rotations about the $^*CH(CH_3)$–O bond, as illustrated in Fig. 7*c*. When $\phi_2 = -49.71°$, the most stable conformation results. Then the interactions of the front, backbone $-CH_2-$ group with the $-CH_3$ group and the rear, backbone $-CH_2-$ group, are minimised. The statistical-weights matrix for fragment 3*R* has high-energy minima at $\phi_2 = \phi_{g+} = 110.20°$, although the statistical weights are very low. However, as can be seen from Fig. 6, the energy of the trans state, $\phi_2 = 0°$, is in fact lower than that of the g_+ state, although the surface has no minimum at $\phi_2 = 0°$. Overall, the increase in energy $E_{g-} < E_t < E_{g+}$ follows the decreasing distances between the front $-CH_2-$ group and the rear $-CH_2-$ and $-CH_3$ groups. At ϕ_{g+}, both the rear groups are close to the front $-CH_2-$ group; at ϕ_t, the rear $-CH_3$ group is close; and at ϕ_{g-}, both the rear groups are approximately equidistant from the front $-CH_2-$ group.

Considering the *S* stereoisomeric forms of $^*C$, the most stable bond-conformations for the fragments are, as expected, mirror-images of those for the *R* isomers. See Fig. 7*d* for fragment 3. For isotactic POP chains of all *R*, or all *S* forms of $^*C$, and for the syndiotactic chain (-*R*-*S*-*R*-*S*-), the sets of ϕ_2 angles of lowest net energy are as follows.

isotactic — O — CH_2 — ^{R}CH(CH_3) — O — CH_2 — ^{R}CH(CH_3) — O —
–3.11° 111.31° –49.71° –3.11° 111.31° –49.71°

isotactic — O — CH_2 — ^{S}CH(CH_3) — O — CH_2 — ^{S}CH(CH_3) — O —
–2.56° –111.31° 49.67° –2.56° –111.31° 49.67°

syndiotactic — O — CH_2 — ^{R}CH(CH_3) — O — CH_2 — ^{S}CH(CH_3) — O —
–2.56° 111.31° –49.71° –3.11° –111.31° 49.67°

The values of ϕ_2 for gauche rotational-states of the *R* and *S* forms are of equal magnitude and opposite sign. (The small differences in absolute values almost certainly arise as a result of errors in the detailed numerical analysis of potential-energy minima). The preferred, trans rotational-state, centred at the O–CH_2 bond is $\phi_2 \approx -3°$ for both *R* and *S* isomers.

Returning to the energy-contour maps in Fig. 5, it is evident that the presence of the $^*C$-atom affects the rotational energies of four-skeletal-bond sequences, such that the *R* and *S* forms of the contour maps are related by a symmetry transformation – a reflection about zero or the average value of the two trans ϕ_1 angles (if they exist), together with a reflection about zero or the average of the two trans ϕ_2 angles (if they exist). This is in agreement with the established relationship[2] between the statistical-weight matrices, $\boldsymbol{U}_R$ and $\boldsymbol{U}_S$, for *R* and *S* forms, respectively, of a given chain fragment:

$$\boldsymbol{U}_R = \boldsymbol{Q}\,\boldsymbol{U}_S\,\boldsymbol{Q} \quad , \tag{8}$$

where

$$\boldsymbol{Q} = \begin{bmatrix} 1\,0\,0 \\ 0\,1\,0 \\ 0\,0\,1 \end{bmatrix} . \tag{9}$$

Simulation of the Conformational Properties of POP Chains

The statistical weights calculated for the *R* and *S* forms of the POP-chain repeating-fragment were used in R-I-S calculations to evaluate C_n for isotactic (chosen as *-S-S-S-S-*) and syndiotactic (*-R-S-R-S-*) POP chains of 15 to 150 skeletal bonds, at a temperature of 353 K. The R-I-S algorithm employed[7] by the BIOSYM software's "R-I-S module" to calculate $\langle r^2 \rangle$, is based on Flory's matrix method[2]. The values of $\langle r^2 \rangle$ found were converted to C_n using Eq. (*1*). For computational efficiency, POP chain-structures of five units (RUs) were defined initially, and calculations carried out for increasing chain-lengths based on multiples of the five-RU structure.

Atactic chain-structures cannot be generated by defining a repeating chain-structure without introducing a degree of regularity in the sequence of *R* and *S* *C-atoms. Hence, an alternative (although more computationally intensive) method was used. For each of fifteen chain-lengths selected between n = 15 and n = 3 000, a Monte-Carlo (M-C) method was used to generate a small, random sample of five atactic POP chains. A higher maximum chain-length (n = 3 000) was used in the atactic-chain analysis in order to investigate the convergence of the calculated values of C_n with increasing n and allow comparison with experimental data (see later). Using the BIOSYM oftware's "Polymerizer module" (ref.[7]), each random, atactic chain-structure was built RU-by-RU, by predefining a 50% chance of choosing a meso diad (*R-R* or *S-S*), or racemic diad (*R-S* or *S-R*), for the addition of each RU. The value of C_n for each completed chain-structure was then calculated, as for the isotactic and syndiotactic chains, using the "R-I-S module" and the set of statistical weights given earlier. The values of C_n for the five chains for each n were averaged.

RESULTS AND DISCUSSION

The characteristic ratio, C_n, is plotted in Fig. 8 as a function of the number of skeletal bonds, n, for isotactic and syndiotactic chains. It is immediately obvious that, due to the cumulative effects of the differences between *R* and *S* forms of *C, the two stereospecific forms of the POP chain display vastly different conformational behaviours. The isotactic chains always have higher values of C_n than the syndiotactic chains.

Hence the latter are expected to be more highly coiled than the former. The corresponding plots of C_n vs the reciprocal number of skeletal bonds, $1/n$, in Fig. 9, are approximately linear, allowing the limiting behaviour of C_n with increasing chain-length to be defined. By extrapolation to $1/n \to 0$, the approximate values of C_∞ for isotactic and syndiotactic POP chains at 353 K are found to be 7.5 and 3.7, respectively. The large

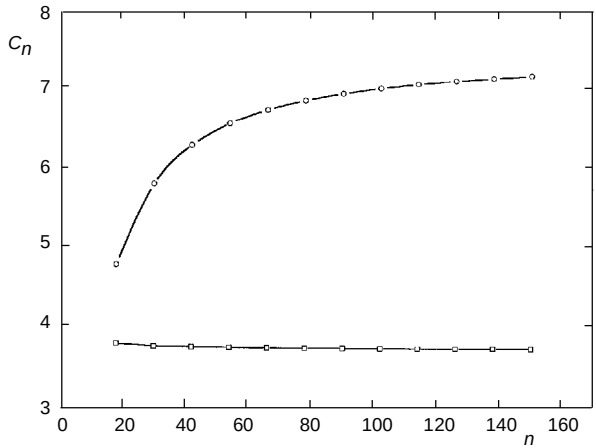

FIG. 8
Characteristic ratio, C_n, at 353 K, as a function of the number of skeletal bonds, n, for isotactic (○) and syndiotactic (□) POP chains of up to 150 skeletal bonds

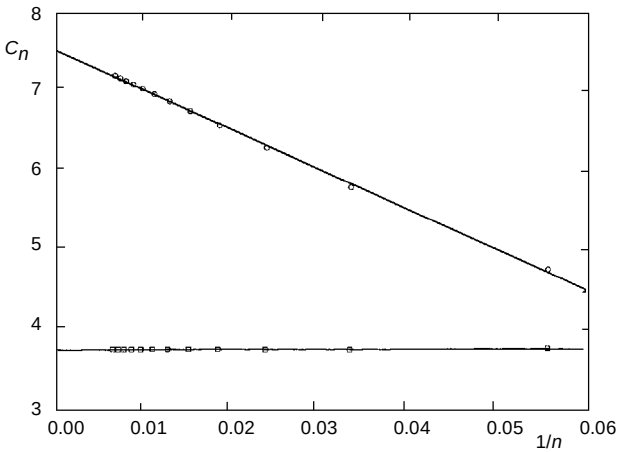

FIG. 9
Characteristic ratio, C_n, at 353 K, as a function of the reciprocal of the number of skeletal bonds, $1/n$, for isotactic (○) and syndiotactic (□) POP chains of up to 150 skeletal bonds

difference in conformational character is illustrated pictorially in Fig. 10, where isotactic and syndiotactic POP chains, each consisting of 10 RUs, have been put in their lowest-energy conformations (using the low-energy sets of dihedral angles, listed previously). The highly-coiled nature of the lowest-energy syndiotactic chain, relative to the more extended nature of the corresponding isotactic chain, is apparent.

The values of C_n for the random, atactic POP chains are plotted alongside those for isotactic and syndiotactic chains in Fig. 11. The error bars indicate the scatter in the five values of C_n calculated for each number of skeletal bonds, due to the random occurrence of the *R* and *S* forms of *C. It is evident that the scatter in C_n decreases with increasing *n*, because, as the number of skeletal bonds increases, the larger set of *R* and *S* *C-atoms in each chain begins to describe better the "average" atactic chain. The least-squares line is plotted using the mean value at each reciprocal chain-length, and extrapolation to $1/n = 0$ yields a value of $C_\infty \approx 5.4$ for the random, atactic POP chain of an infinite number of skeletal bonds. This value is approximately the average of the two C_∞ values for isotactic and syndiotactic POP chains, quoted earlier.

Although not described in detail in this paper, a similar set of R-I-S calculations were carried out to analyse the same series of atactic POP chains of different lengths at a

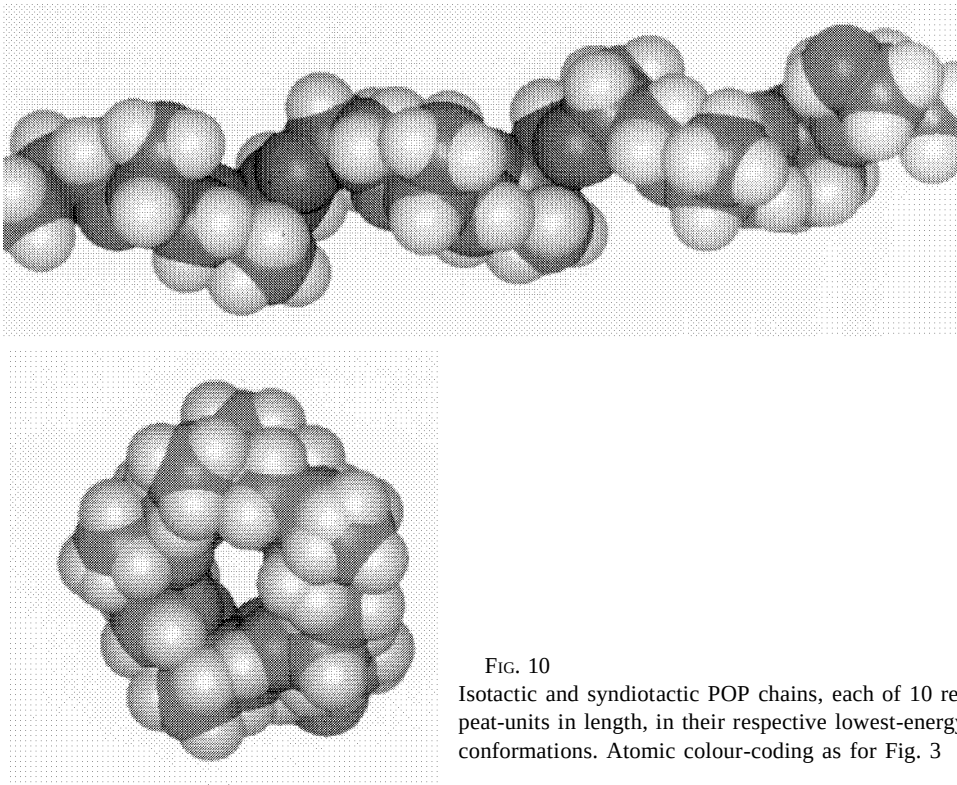

FIG. 10
Isotactic and syndiotactic POP chains, each of 10 repeat-units in length, in their respective lowest-energy conformations. Atomic colour-coding as for Fig. 3

temperature of 333 K (to coincide with an experimental polymerisation temperature[1]). The extrapolated value of C_∞ in this case was found to be ≈5.5, allowing the value of the temperature coefficient, $d(\ln \langle r^2 \rangle)/dT \approx -0.92 \cdot 10^{-3}$ K^{-1}, to be calculated. The corresponding values of $d(\ln \langle r^2 \rangle)/dT$ for isotactic and syndiotactic POP chains were found to be $-2.2 \cdot 10^{-3}$ K^{-1} and $1.3 \cdot 10^{-3}$ K^{-1}, respectively.

Examples of typical conformations (whose end-to-end distances are approximately equal to $\langle r^2 \rangle^{1/2}$) for isotactic, syndiotactic and atactic POP chains, using the current model, and consisting of twenty RUs, were generated using BIOSYM's "R-I-S Monte-Carlo module" (ref.[7]). The R-I-S Monte-Carlo method, in which conditional probabilities are assigned to pairs of sequential dihedral angles, is based on a method described elsewhere[11] and provides a means whereby chain-conformations can be built bond-by-bond at random, in proportion to their total probability of occurrence. Three typical POP chain conformations are shown in Fig. 12. The extended form of the isotactic POP chain relative to the more coiled syndiotactic chain is again evident. The random, atactic POP chain appears less coiled than the syndiotactic chain, although not as extended as the isotactic chain, as expected.

Correlation with Experimental Data and Previous R-I-S Calculations

The unperturbed dimensions of POP chains have been measured by Allen, Booth, Price and Jones[5,6]. High-molar-mass POP was prepared using a zinc diethyl–water catalyst, and fractions with varying (but unknown) degrees of isotacticity, were analysed using

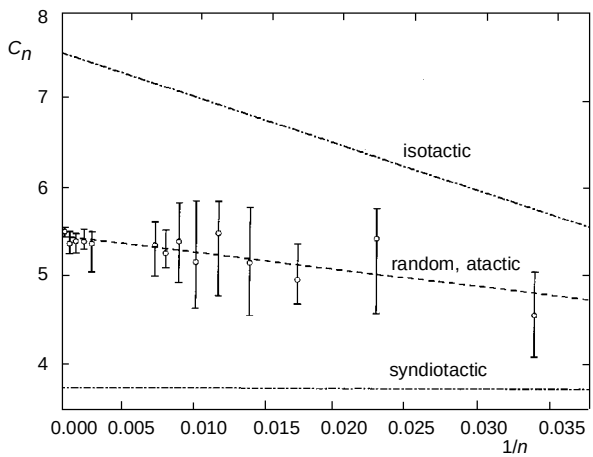

FIG. 11

Characteristic ratio, C_n, at 353 K, as a function of the reciprocal of the number of skeletal bonds, $1/n$, for random, atactic POP chains of up to 3 000 skeletal bonds. The error bars indicate the ranges of C_n values associated with the samples of five atactic chains analysed for each n

viscometry and light-scattering. The latter method, in which isooctane at the Θ-temperature (50 °C) was used as the solvent, is expected to yield the most reliable values of $\langle r^2 \rangle$, and hence C_∞ (via Eq. (*1*)). The C_∞-values thus calculated for the series of POP fractions lie in the range 5.26–6.73. The upper and lower values of C_∞ correspond to the POP fractions with higher and lower degrees of isotacticity[6], respectively. (It should be noted that a low degree of isotacticity corresponds to a high degree of atacticity.) Additionally, the dilute-solution properties of low-molar-mass POP diols, and polyurethanes derived from them, were investigated by Moacanin[12]. The diols had molar masses 2 025 and 1 025 g mol^{-1}, giving $n \approx 105$ and $n \approx 53$, respectively. They were commercially produced by base catalysis, and were therefore probably atactic. Analysis of the measured values of the intrinsic viscosities of POP diols 2 025 at 39.5 °C, and 1 025 at 25 °C, yields values of $C_{105} = 5.1$ and $C_{53} = 4.7$, respectively.

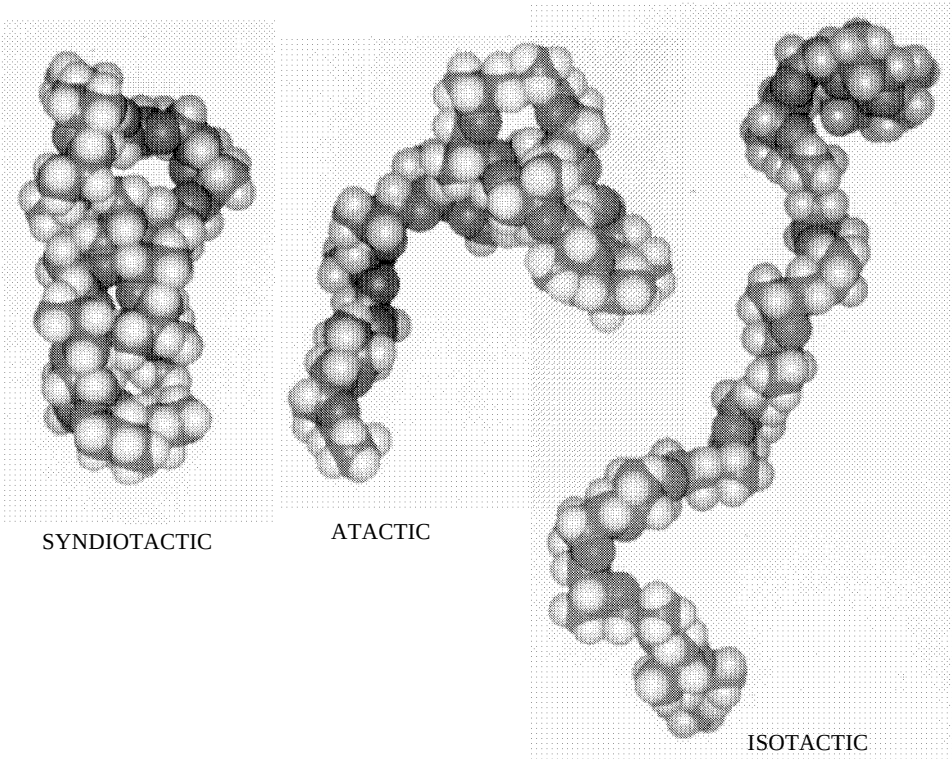

FIG. 12
Typical conformations of isotactic, syndiotactic and atactic POP chains of twenty repeat-units at 353 K. Each chain conformation was generated using BIOSYM's R-I-S Monte-Carlo procedure[7]. Atomic colour-coding as for Fig. 3

In Fig. 13, the experimental values of C_∞ (from Allen et al.[5,6]), C_{105} (Moacanin, see ref.[12]) and C_{53} (Moacanin, see ref.[12]) have been scaled using the $d(\ln \langle r^2 \rangle)/dT$ value for atactic POP calculated above, for direct comparison with the calculated values of C_n at 353 K. It is clear that the calculated values of C_∞ for atactic POP from the present work show a good correlation with the experimentally-determined values. Without empirical adjustment of the R-I-S energy-parameters and dihedral angles, the experimental chain-length dependence of C_n is reproduced, although the calculated values appear to be about 10% higher than the experimental values. The observed increases in C_∞ with increasing isotacticity are also predicted by the current model.

A predominantly isotactic (…-*R*-*R*-…) POP sample was analysed by Hirano, Khanh and Tsuruta[13], using NMR spectroscopy. More specifically, the proportions of g^-, t and g^+ rotational states about the C–*C bond at 298 K were found to be 0.1, 0.4 and 0.5, respectively. The ratio $g^- : t : g^+$ of 0.19 : 0.33 : 0.48 for the current model (see fragment 2*R*) at 298 K is in reasonable agreement with the experimental observations. These authors also comment on the suppression of the g^- state, due to the triple-steric-interaction between the two skeletal –O– atoms and the $–CH_3$ side-group (see Fig. 7*b*).

The values of C_n for isotactic, atactic and syndiotactic POP chains of 300 bonds, calculated by Abe et al.[4], are also shown in Fig. 13. They have been scaled to 353 K using Abe's temperature coefficients[3], of $–1.59 \cdot 10^{-3}$ K^{-1}, $–0.25 \cdot 10^{-3}$ K^{-1} and $0.64 \cdot 10^{-3}$ K^{-1}, respectively, for isotactic, atactic and syndiotactic chains. It can be seen that the R-I-S parameters, semi-empirically chosen to yield a value of $C_{300} = 6.0$ for isotactic POP at 323 K, also predicts an increase in C_n with increase in the degree of isotacticity. The

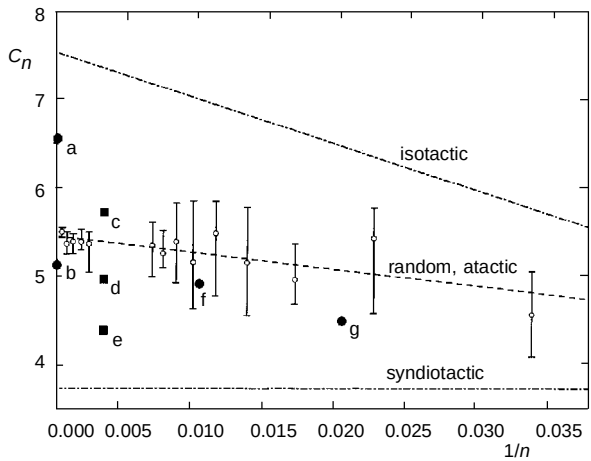

FIG. 13

Experimental values of C_∞ and C_n, and the predictions of C_n made by Abe et al.[4], compared with the results presented in Fig. 11, for the current R-I-S model: a upper experimental value[5,6]; b lower experimental value[5,6]; c isotactic[4]; d atactic[4]; e syndiotactic[4]; f,g atactic[12]

prediction of C_∞ for atactic POP chains is (by chance) in good agreement with experiment. However, it appears that C_∞ for isotactic POP is underestimated relative to experiment, and the range of C_n values, in going from isotactic to syndiotactic chains, is smaller, compared with the current model.

A more detailed comparison of experimental measurements of the unperturbed dimensions, dipole moments and proportions of C–*C rotational states (from NMR) with the predictions from various R-I-S models (Abe et al.[4], Ishikawa and Teramoto[14]), and those from R-I-S calculations using different forcefields is currently being made. This work will be reported in a future publication.

The support of the EPSRC (Grant No. GR/J/24935), and also of Biosym Technologies is gratefully acknowledged. D.J.R.T. wishes to thank the staff of the UMIST Computing Support Unit, and R. Nutter of the Department of Computation, UMIST.

REFERENCES

1. Stepto R. F. T. in: *Comprehensive Polymer Science* (S. L. Aggarwal and S. Russo, Eds), 1st Suppl., Chap. 10. Pergamon Press, Oxford 1992.
2. Flory P. J.: *Statistical Mechanics of Chain Molecules*. Interscience, New York 1969.
3. Brandrup J., Immergut E. H. (Eds): *Polymer Handbook*, 3rd ed. Wiley, New York 1989.
4. Abe A., Hirano T., Tsuruta T.: Macromolecules *12*, 1092 (1979).
5. Allen G., Booth C., Jones M. N.: Polymer *5*, 257 (1964).
6. Allen G., Booth C., Price C.: Polymer *7*, 167 (1966); *8*, 397 (1967).
7. Biosym Technologies Inc.: *Discover Version 2.9.5 and 94.0, User Guide, Part 1*. San Diego 1994; *Polymer Version 6.0, User Guide*, Parts 1 and 2. San Diego 1993.
8. IUPAC: *A Guide to IUPAC Nomenclature of Organic Compounds, Recommendations 1993*, pp. 152–154. Blackwell Scientific Publications, Oxford 1993.
9. Young R. J., Lovell P. A.: *Introduction to Polymers*, 2nd ed., p. 102. Chapman–Hall, London 1991.
10. Abe A., Mark J. E.: J. Am. Chem. Soc. *98*, 6468 (1976).
11. Hill J. L., Stepto R. F. T.: Trans. Faraday Soc. *67*, 3202 (1971).
12. Moacanin J.: J. Appl. Polym. Sci. *1*, 272 (1959).
13. Hirano T., Khanh P. H., Tsuruta T.: Makromol. Chem. *153*, 331 (1972).
14. Ishikawa T., Teramoto A.: Polym. J. *6*, 207 (1974).